*35th EPS Conference on Plasma Phys. Hersonissos, 9 - 13 June 2008 ECA Vol.**32D**, P-2.151 (2008)*

Electron generation in femtosecond laser heated dielectrics

C. Mézel[1], A. Bourgeade[2], L. Hallo[1], O. Saut[3]

[1] *CELIA, Université Bordeaux 1, France*

[2] *CEA-CESTA, Le Barp, France*

[3] *IMB, Université Bordeaux 1, France*

Introduction

Interaction of sub-picosecond laser pulses with transparent dielectrics is a fast growing domain of material processing, which opens a way to release energy inside a material so that interaction takes place in a confined geometry. Recent experiments [1, 2], showed possibility to focus the laser pulse into a spot of size of a few tenths of laser wavelength by using a microscope objective with a high numerical aperture. The deposited energy produces a micro explosion, a diverging shock wave within the bulk and a cavity formation.

Two self-consistent, 2D and 3D models have been developed for such application. First one is a global model based on Penano's work [3] which includes multiphoton and collisionnal ionisation, and a recombination time for electrons. But the local thermal equilibrium assumption is known to be valid only for long laser pulse duration. A new multigroup (MG) model based on Rethfeld work [4] has been developed and complemented by energy and density balances between groups. It enables to compute accurately the energy transfered from laser to electrons in the conduction band.

Electromagnetic calculations of the laser energy deposition are carried out in 2D and 3D geometries, including Kerr effect, multiphoton and electron collision ionisation processes. Final spatial energy distribution in the focal zone is found to be sensitive to the ionisation process drived by local energy of the groups.

Process of laser energy release with global model

For laser pulse durations shorter than the hydrodynamic response time, one can assume that atoms are at rest and only the electron dynamics needs to be considered. A tight focusing creates strongly nonlinear propagation conditions even for a small laser pulse energies of a few tens of nJ. Such phenomena as a strong diffraction, or dispersion and plasma formation can be invoked. Modeling of sub-wavelength laser focusing requires solution of a full set of Maxwell's equations

coupled to equations describing a non-linear response of the matter:

$$\nabla \times \vec{E} = -\frac{\partial \vec{B}}{\partial t}, \quad \nabla \times \vec{H} = \frac{\partial \vec{D}}{\partial t} + \vec{J} + \vec{J}_{mpi}. \tag{1}$$

$\vec{J}$ is the electric current computed with Drude model:

$$\partial_t \vec{J} = -\nu_e \vec{J} + e^2 n_e \vec{E}/m_e, \tag{2}$$

where n_e is the density of free electrons, and $\nu_e = \nu_{ei} + \nu_{en}$ is the effective electron collision frequency with neutrals and ions. $\vec{J}_{mpi}$ is the effective current accounting for multiphoton ionisation (MPI). It is obtained through a balance on the power loss ($\partial U_{mpi} = -\vec{J}_{mpi}.\vec{E}$) and the power gain ($\partial U_{mpi} = W_{ion}\nu_{mpi}n_n$), which leads to the following expression:

$$\vec{J}_{mpi} = -\frac{\vec{E}}{|\vec{E}|^2} W_{ion} n_n \nu_{mpi}, \tag{3}$$

where W_{ion} is the ionisation energy of the material (9 eV for silica and 8.8 eV for sapphire). The ionisation probability by N-photon absorption reads

$$\nu_{mpi}[sec^{-1}] = \frac{\sigma_N I^N}{n_{n0}}, \tag{4}$$

where I is the laser intensity and σ_N is the effective ionisation cross section. For the case of Ti-Sa laser ($\lambda = 800$ nm) and silica, $N = 6$ photons and $\sigma_6 \approx 2 \times 10^{13}$ cm^{-3}psec^{-1}(cm^2/TW)^6 [3].

Maxwell's equations are complemented with a free electron density n_e evolution equation:

$$\partial_t n_e = \nu_{mpi} n_n + \nu_{col} n_e - n_e/\tau_{rec}, \tag{5}$$

where n_n is the number of neutrals. The right hand side accounts for the MPI and collisional ionisation and for the radiative recombination due to the electron trapping [3]. The $\nu_{col}(n_n, T_e)$ term was evaluated using a maxwellian electron distribution function.

Typical focal volumes are calculated assuming that these volumes are ellipsoidal. The axis dimensions are determined by the points around the maximum on the propagation and transverse directions where the absorbed energy reaches half of its maximum. A typical energy distribution obtained for 40 TW/cm^2 in silica is presented in Fig. 1., with a normalisation in fraction of the total initial laser energy. The absorption volume is a 0.5 μm^3 ellipsoidal volume located at a depth of 2 μm under the computational domain surface. Energy is deposited in a very small volume which enables the obtention of a very important absorbed energy density: about 200 kJ/cm^3. About 10% of the atoms are ionised, which leads to a free electron density of 1.5 10^{21}cm^{-3}.

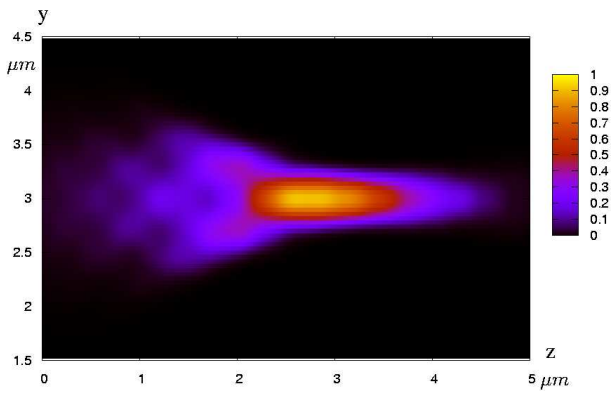

Figure 1: Absorbed energy contours in silica after a 180 fs, 27 nJ laser energy shot

.

Enhancement of the energy distribution: multigroup model

The assumption of thermal equilibrium for electrons is thought to be no longer valid for short laser pulses because the characteristic variation time of the laser energy release in the matter is shorter than the electron-electron collision time. Hence, there is not enough time for the electrons to get back to a Maxwellian regime. For this reason, a new model based on Rethfeld's work has been developed. Electrons are now shared between different energy groups in the conduction band (CB) according to their kinetic energy, which allows to obtain faster the thermal equilibrium.

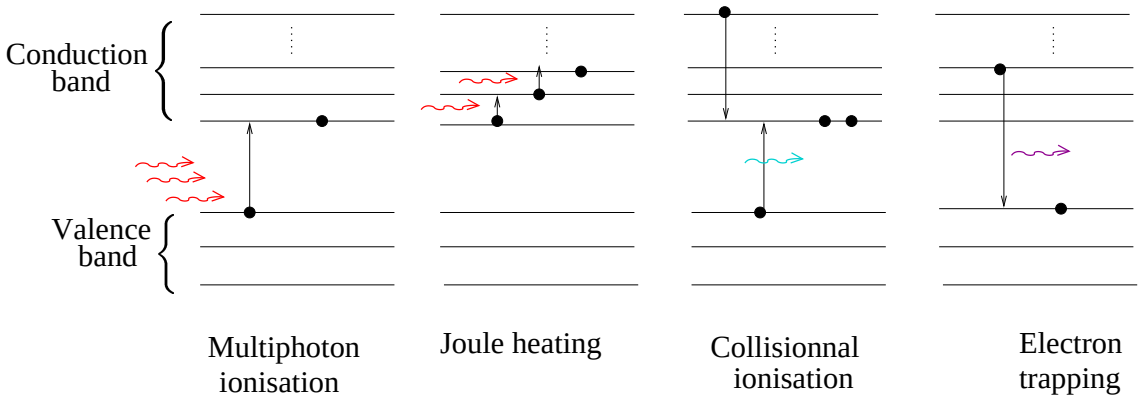

Figure 2: Scheme of the mechanisms occuring in the valence and conduction bands

Ionisation mechanisms are presented in Fig. 2., and several assumptions are made for a better understanding of the process:

- Multiphoton ionisation produces electrons in the first group of the CB only.
- Electrons are accelerated in the laser field by ohm effect

- Collisional ionisation involves only high energetic electrons (from the last group of CB)
- Electron trapping occurs for each group of the CB and produces electrons in the last group of the Valence Band.

A 2D comparison of the two models is shown if Fig. 3. for a $\lambda = 800$ nm, 100 fs and 135 nJ laser shot. The beam waist is rather large, $\omega_0 = 2\ \mu$m, which ensures a surfacic absorption.

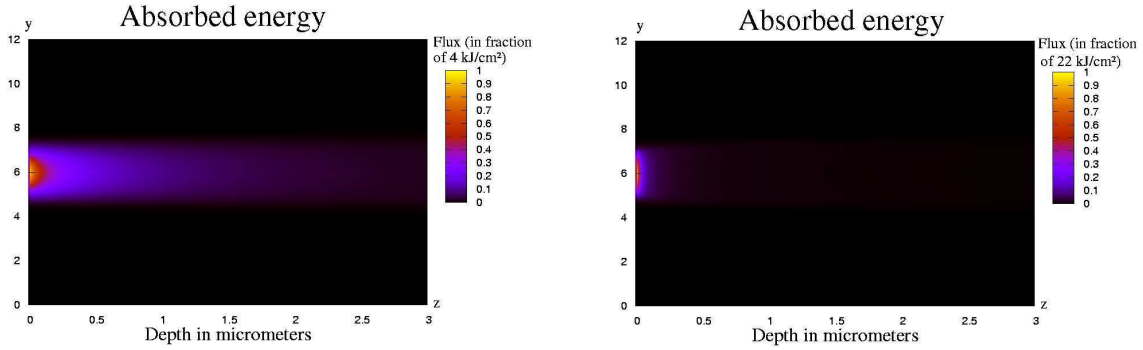

Figure 3: Absorbed energy in fraction of initial laser energy after a 100 fs, 135 nJ laser energy shot on depth. Left: computation with global model. Right: computation with MG model.

Absorbed energy is found to be higher and more localised in case of MG model. Indeed, the absorption length is longer with the global model ($l_a \approx 200$ nm) than with the MG model ($l_a \approx 100$ nm) and the maximum absorbed energy is 4 kJ/cm^2 with the global model, and 22 kJ/cm^2 with the MG model.

Other results show that ionisation begins faster with the global model but is more efficient in case of MG model. This is due to the collisionnal ionisation which is used more accurately in the MG model, as only high energetic electrons can perform it.

References

[1] S. Juodkazis et al., Phys. Rev. Let. 96 166101 (2006)

[2] E. Gamaly et al., Current Applied Physics 8, issues 3-4, p.412-415 (2008)

[3] J. Penano et al., Phys. Rev. E 72 36412 (2005)

[4] B. Rethfeld, Phys. Rev. Let. 92 187401 (2004)